Current health sciences journal

Curr Health Sci J. 2020 Jul-Sep; 46(3): 290–296. Published online 2020 Sep 30.
doi: 10.12865/CHSJ.46.03.11: 10.12865/CHSJ.46.03.11

PMCID: PMC7716760 | PMID: 33304631

Finite Element Analysis of a Novel Aortic Valve Stent

ŞTEFAN CASTRAVETE,[1] DUMITRU MAZILU,[2] LUCIAN GHEORGHE GRUIONU,[3] CRISTIAN MILITARU,[4,6] SEBASTIAN MILITARU,[4,6] ANCA-LOREDANA UDRIŞTOIU,[5] ANDREEA VALENTINA IACOB,[5] and GABRIEL GRUIONU[3,7]

[1]Caelynx Europe Ltd., Craiova, Romania
[2]National Heart, Lung and Blood Institute, National Institutes of Health, Bethesda, MD, USA
[3]Faculty of Mechanics, University of Craiova, Romania
[4]Cardiomed Ltd.
[5]Faculty of Automation, Computers and Electronics, University of Craiova, Romania
[6]Faculty of Medicine and Pharmacy of Craiova, Romania
[7]Krannert Cardiovascular Institute, Department of Medicine, Indiana University School of Medicine, Indianapolis, Indiana, USA
Corresponding Author: Gabriel Gruionu, Faculty of Mechanics, University of Craiova, Craiova, Romania, Krannert Cardiovascular Institute, *Department of Medicine,* Indiana University School of Medicine, Indianapolis, Indiana, USA, gruionu@gmail.com

Received 2020 May 15; Accepted 2020 Sep 24.

Abstract

Worldwide, one of the leading causes of death for patients with car
disease is aortic valve failure or insufficiency as a result of calcifica

cardiovascular disease. The surgical treatment consists of repair or total replacement of the aortic valve. Artificial aortic valve implantation via a percutaneous or endovascular procedure is the minimally invasive alternative to open chest surgery, and the only option for high-risk or older patients. Due to the complex anatomical location between the left ventricle and the aorta, there are still engineering design optimization challenges which influence the long-term durability of the valve. In this study we developed a computer model and performed a numerical analysis of an original self-expanding stent for transcatheter aortic valve in order to optimize its design and materials. The study demonstrates the current valve design could be a good alternative to the existing commercially available valve devices.

Keywords: Aortic valve, stent, finite elements, nitinol

Introduction

The aortic valve allows the oxygenated blood from the heart's right ventricle to flow into the aorta and the arterial system and prevents blood from flowing back into the ventricle. To reduce trauma and recovery period of the patient, aortic valve replacement can be performed transapically, in a procedure that provides a direct access to the natural valve, using real-time MRI for intraoperative guidance and results assessment [1,2].

During these procedures, the valve is attached to a stent and delivered via a catheter to the anatomical location. The stent is expanded and fixed in place via specific stent features.

The function of the aortic valve is complex, with a durability of the bioprosthetic valves between 12 to 15 years. The functional limitations are the mechanical properties of the valve and the effect of the stresses imposed on the valve leaflets by the stent structure, while the aortic root to which the artificial valve is attached expands and contracts during the cardiac cycle.

An important feature of the natural heart valve is its ability to expand in diameter by more than 10% during systole which facilitates the flow of blood and contributes to minimal bending of the cusps, and reduced internal flexural fatigue [3].

There is also a meaningful torsion/twisting motion that the aorta endures during

each pulse. All these motions need to be considered in the design of a valve stent which will be attached to the aortic wall. The stent has specific design to ensure its resilience, durability, and ability to be delivered transapically and repositioned in a patient, while providing an appropriate opening of the valve during systole to facilitate blood flow, and minimal bending of the cusps to reduce valve failure.

Other important features of a stent are to: slightly expand during compression but not apply too much force to the valve leaflets, provide a stable yet flexible scaffolding platform for the valve prosthesis, resist torsion, also be able to expand and contract repeatedly over long periods of time [4,5].

Material and Methods

Aortic Valve Stent Design

The present aortic valve design includes an expandable stent to support the prosthesis and to anchor the prosthesis to the aortic root. The patented [6], self-expandable stent, designed for a 25mm diameter aorta, includes a tubular lattice structure defined by longitudinally aligned rods connected to V-shaped struts and present flares along opposite ends of each rod to properly seat and prevent undue torsion during deployment and placement within the lumen (Figure 1a). Attached to the stent is an equine or bovine pericardial trileaflet valve (Figure 1b)

Finite Element Model

The assembly of the aorta, aortic valve and stent is modeled with solid finite elements using the software package Abaqus (Dassault Systemes, Paris, France). The aorta and stent are modeled with 1st order C3D8I hexahedral elements. The C3D8I incompatible mode elements are hexahedral elements which minimize the appearance of hourglass modes as well as the node lock phenomenon. The valves and valve cage are modeled with modified 2nd order tetrahedral elements, C3D10M [3].

Boundary conditions and loads

Two loading cases were considered:

1: Uniform pressure of 4.4kPa applied to the lower surface of the valve (Figure 3, a)

to test the strength of the valve opening.

2: Constant blood flow with a speed of 4l/min to open the valve and deform the stent and the aorta

Stent material

The material used to model the stent was Nitinol [7,8,9,10].

The Abaqus material subroutines was employed to simulate its behavior with the following values (Table 1).

For valves, valve cage and aorta an hyperelastic material model Ogden 2nd order [11,12] was used. Ogden strain energy potential is given by [7]:

where $\bar{\lambda}_i$ represent deviatoric principal stretches; N is the order of approximation; and μ_i, α_i , and D_i are parameters which depend on temperature. The initial shear modulus and bulk modulus are:

The resulting stress-strain curve from the Ogden 2nd order material model is shown in Figure 4.

In this study, the density of the leaflet was 1100kg/m^3, α_1=67.74, α_2=27.47, μ_1=19.58kPa, μ_2=260.56kPa [13].

Blood was modeled as an inviscid fluid [4] with 1060Kg/m^3 density and 0.0035 Pa s dynamic viscosity.

Fluid structure interaction case is modeled as smooth particle hydrodynamics (SPH). SPH is a Lagrange system where the fluid is represented by a discrete set of points distributed over the domain with no need to discretize the domain into elements.

The Lagrange method correlated with the non-existence of a fixed mesh is used to model the complexity correlated with fluid modeling, large displacement structural problems and free surfaces [7].

The method is a representation of continuum partial differential equations. In that

regard, smoothed particle hydrodynamics is like the finite element method. Like FEA, SPH uses an interpolation method to approximate a field variable at any point in a domain. The contributions of neighboring particles give the output of a variable in a form of summation:

where the “kernel” function, W, is different than zero.

Results

The stress distribution for the valve leaflets and stent (Figure 5), as well as the radial (Figure 6) and axial deformations (Figure 7) were computed to evaluate the biomechanical state for constant blood flow (4L/min) which opens the valve. The maximum von Mises stress (0.26MPa) is distributed at leaflet base and at opposite end of the stent (17MPa).

The radial (0.18mm) and axial (0.26mm) maximal deformations for the stent were proved to be relatively small because of the particular design of the stent with longitudinally rods connected to V-shaped struts, developing an increase resilience and durability and reducing the valve failure due to the minimal bending of the cusps.

Discussion

Cardiovascular disease is the leading cause of death world-wide with important economic implications [14].

Transcatheter valve replacement is an alternative treatment to surgery for stenosis of aortic valves [15], when the diseased valve is replaced by a biological valve sutured to a stent, deployed using a catheter through the femoral artery to its natural position in the body.

The stent used in this procedure as a support structure has a great importance, enduring high stress due to the blood flow changes in the heart. This paper presents the design of a novel, patented stent, with a design to increase its rigidity, that was analyzed using finite element method with Abaqus software, under natural loading conditions. Similar other studies have analyzed stent design for aortic or mitral valve application [16,17].

A possible next step for our study would be to use explanted swine heart and aortic arch tissue to test the aortic valve stent as other groups tested the mitral valve stent [16].

This will further validate our theoretical results. Another necessary study is to analyze the effect of calcification plaque on the aortic wall stress distribution and how the stent will alleviate this stress [17].

Two testing scenarios were used: one for pressure loading on the valve to maintain the valve closed, and the second one when there is a constant flow of blood to open the valve [11,13].

In both cases we calculated the deformations and stresses in the stent in the radial and axial directions. In the radial direction, there was a larger deformation in the first case scenario when the stent has to hold the valve closed. In the second scenario when the valve is open, the stent undergoes negative radial deformations where the valve is attached (stent is pulled slightly inward when the valve opens) but overall the deformation is smaller than in the first scenario.

In the axial direction, the deformations are larger than in the radial direction (but still within the normal limits) to accommodate the torsion/twisting motion of the aorta and slightly reposition in the patient. The particular, V shape of the stent's struts allows deformation of the stent without changing its shape and durability. Because of this particular design, the stent undergoes small deformations resulting in a reduced fatigue of the valve failure due to the minimal bending of the cusps, but the peak stresses for leaflets located at the line of junction will possibly produce a leaflet degeneration in these regions.

For the valve and stent ensemble, the stresses in the valve were in the same range but slightly higher in the pressure load scenario which shows that the features of a stent do not apply too much force to the valve leaflets. The stresses on the stent struts show a few points of increased stress at the tip of the V shape but overall, they offer a stable yet flexible scaffolding platform for the valve prosthesis which expand and contract repeatedly over time.

Conclusions

The finite element method is an important tool to precisely analyze the design and the performance of the medical devices [18], and particularly of an aortic valve mounted on an original stent for this study.

During analyses, we used two loading cases scenarios to simulate the valve behavior, and compute stress distribution and displacements: a uniform distributed pressure on the valve leaflets and a constant blood flow.

The geometry of the stent with tubular lattice structure defined by longitudinally aligned rods connected to V-shaped struts proved to improve its behavior by reducing the axial displacement under a constant blood flow as reported before [19].

Another improvement of the design will be accomplished by using the patient's own anatomy and optimizing the stent shape and mechanical characteristics [20].

Future modeling scenarios could include more complex boundary conditions like the pulsatile blood flow and three-layer model for aorta wall, or clinical procedures like crimping and balloon expansion during delivery, for a further optimization of the valve design efficiency and durability.

Conflict of interests

None to declare.

Acknowledgments

The research leading to these results has received funding from Competitiveness Operational Program 2014-2020 under the project P_37_357 "Improving the research and development capacity for imaging and advanced technology for minimal invasive medical procedures (iMTECH)" grant, Contract No. 65/08.09.2016, SMIS-Code: 103633.

This work was also partially supported by the grant POCU 380/6/13/123990, co-financed by the European Social Fund within the Sectorial Operational Program Human Capital 2014-2020.

References

1. Horvath KA, Mazilu D, Guttman M, Zetts A, Hunt T, Li M. Midterm results of transapical aortic valve replacement via real-time magnetic resonance imaging guidance. *J Thorac Cardiovasc Surg.* 2010;139(2):424–430. [PMCID: PMC2813338] [PubMed: 19969312]

2. Horvath KA, Mazilu D, Kocaturk O, Li M. Transapical aortic valve replacement under real-time magnetic resonance imaging guidance: experimental results with balloon-expandable and self-expanding stents. *Eur J Cardiothorac Surg.* 2011;39(6):822–828. [PMCID: PMC3038190] [PubMed: 20971017]

3. Xuan Y, Krishnan K, Ye J, Dvir D, Guccione JM, Ge L, Tseng EE. Stent and leaflet stresses in a 26-mm first-generation balloon-expandable transcatheter aortic valve. *J Thorac Cardiovasc Surg.* 2017;153(5):1065–1073. [PMCID: PMC5837867] [PubMed: 28108064]

4. DeHerrera MA, Dang N. Finite Element Analysis of a Percutaneous Stent-Mounted Heart Valve. *Proceedings of the Abaqus Users' Conference.* 2004:209–223.

5. Gideon V, Kumar P, Mathew L. Finite Element Analysis of the Mechanical Performance of Aortic Valve Stent Designs. *Trends Biomater Artif Organs.* 2009;23(1):16–20.

6. Horvath KA, Mazilu D, Li M. Stent for valve replacement. *US Patent App.* 2012;13:265–315.

7. Hibbitt, Karlsson and Sorensen. Abaqus Explicit User's Manual. *Hibbitt, Karlsson and Sorensen Inc.* 2001:996.

8. Yam MCH, Fang C, Lam ACC, Zhang Y. Numerical study and practical design of beam-to-column connections with shape memory alloys. *J Construct Steel Res.* 2015;104:177–192.

9. Kumar GP, Mathew L. Self-expanding aortic valve stent-material optimization. *Comput Biol Med.* 2012;42(11):1060–1063. [PubMed: 22981766]

10. Reedlunn B, Churchill CB, Nelson EE, Shaw JA, Daly SH. Tension compression and bending of superelastic shape memory alloy tubes. *J Mech Phys of Solids.* 2014;63:506–537.

11. Gao B, Zhang Q, Chang Y. Hemodynamic effects of support modes of LVADs on the aortic valve. *Med Biol Eng Comput.* 2019;57:2657–2671. [PubMed: 31707689]

12. Hasan A, Ragaert K, Swieszkowski W, Selimović S, Paul A, Camci-Unal G, Mofrad MR, Khademhosseini A. Biomechanical properties of native and tissue engineered heart valve constructs. *J Biomech.* 2014;47(9):1949–1963. [PubMed: 24290137]

13. Gao B, Zhang Q. Biomechanical effects of the working modes of LVADs on the aortic valve: A primary numerical study. *Comput Methods Programs Biomed.* 2020;193:105512–105512. [PubMed:

32344270]

14. Yusuf S, Hawken S, Ounpuu S, Dans T, Avezum A, Lanas F, McQueen M, Budaj A, Pais P, Varigos J, Lisheng L, INTERHEART Study Investigators Effect of potentially modifiable risk factors associated with myocardial infarction in 52 countries (the INTERHEART study): case-control study. *Lancet.* 2004;364(9438):937–952. [PubMed: 15364185]

15. Lewis G. Materials, fluid dynamics, and solid mechanics aspects of coronary artery stents: a state-of-the-art review. *J Biomed Mater Res B Appl Biomater.* 2008;86(2):569–590. [PubMed: 18240274]

16. Loger K, Pokorny S, Schaller T, Haben I, Frank D, Lutter G. Novel stent design for transcatheter mitral valve implantation. *Interact CardioVasc Thorac Surg.* 2018;26:190–195. [PubMed: 29361168]

17. Jin C, Liu R-H, Zhong S-P, Wang L-Z, Fan Y-B. Effect of Stent Designs on the Paravalvular Regurgitation of Transcatheter Aortic Valve Implantation. *International Journal of Computational Methods.* 2019;16(3):1842007–1842007.

18. Kumar GP, Mathew L. Stent biomaterial and design selection using finite element analysis for percutaneous aortic valve replacement . *Artif Organs.* 2011;35(2):166–175. [PubMed: 21108649]

19. Salemizadeh Pariz F, Mehrabi R, Karamooz-Ravari MR. Finite element analysis of NiTi self-expandable heart valve stent. *Proc Inst Mech Eng [H]* 2019;233(10):1042–1050. [PubMed: 31354047]

20. Hopf R, Gessat M, Russ C, Sündermann SH, Falk V, Mazza E. Finite Element Stent Modeling for the Postoperative Analysis of Transcatheter Aortic Valve Implantation. *J Med Devices.* 2017;11(2):021002–021002.

Figures and Tables

Figure 1

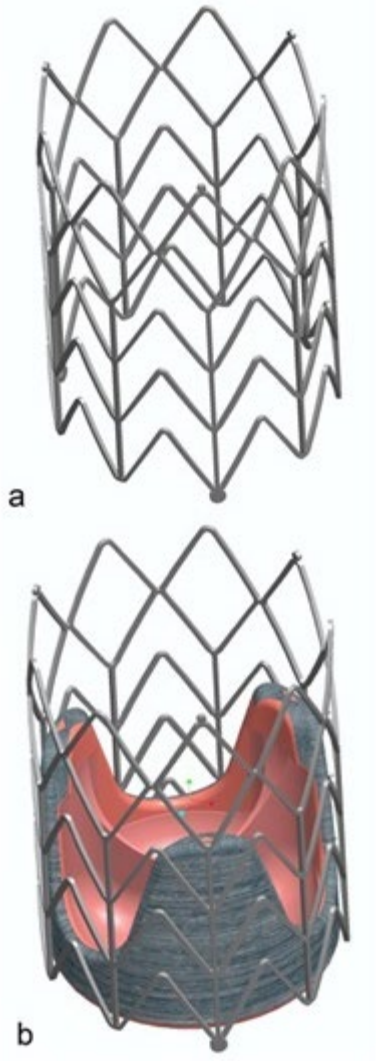

Self-expended original stent (patented) (a) and a trileaflet valve (b)

Figure 2

FEM model assembly (half) (a), aorta (b), valve cage (c), valves (d), stent (e), detailed view of the stent (f).

a.

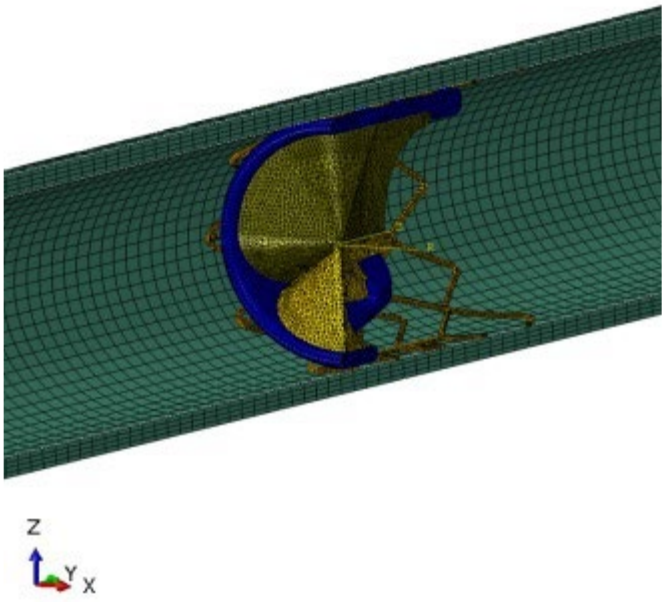

b.

c.

d.

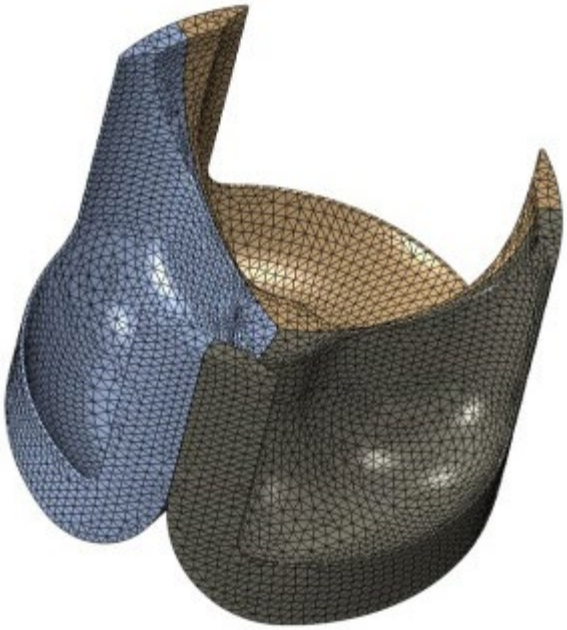

e.

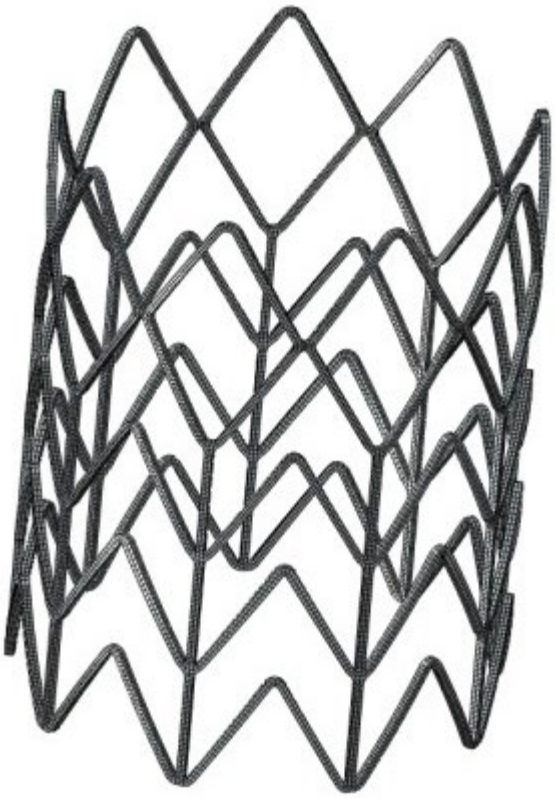

f.

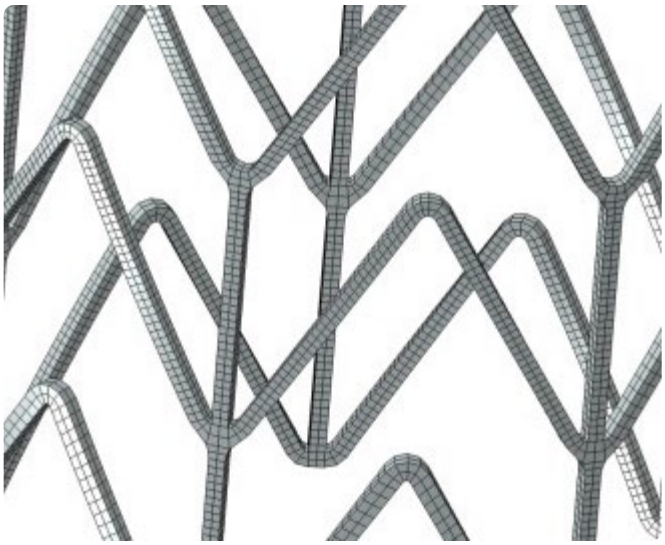

Figure 3

Boundary conditions and loads. (a) pressure load, and fluid (blood) structure interaction (b), opposite pressure applied to the stent flares to cancel axial movement of the stent (c)

a.

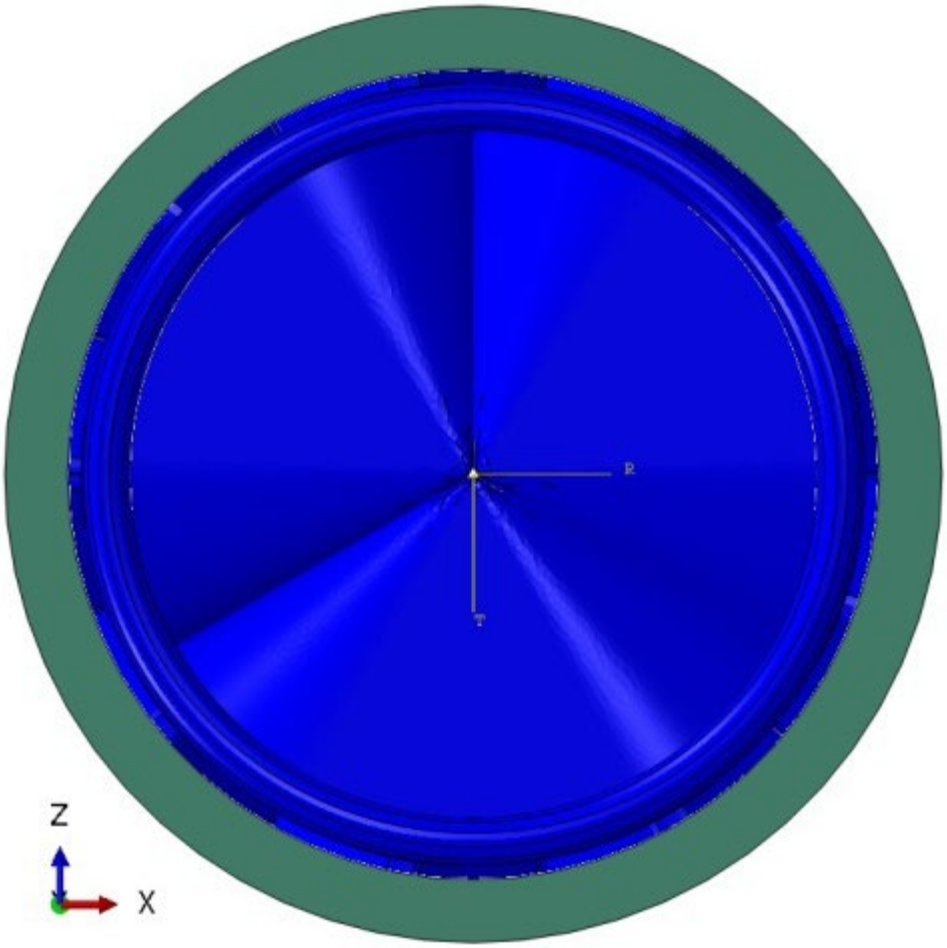

b.

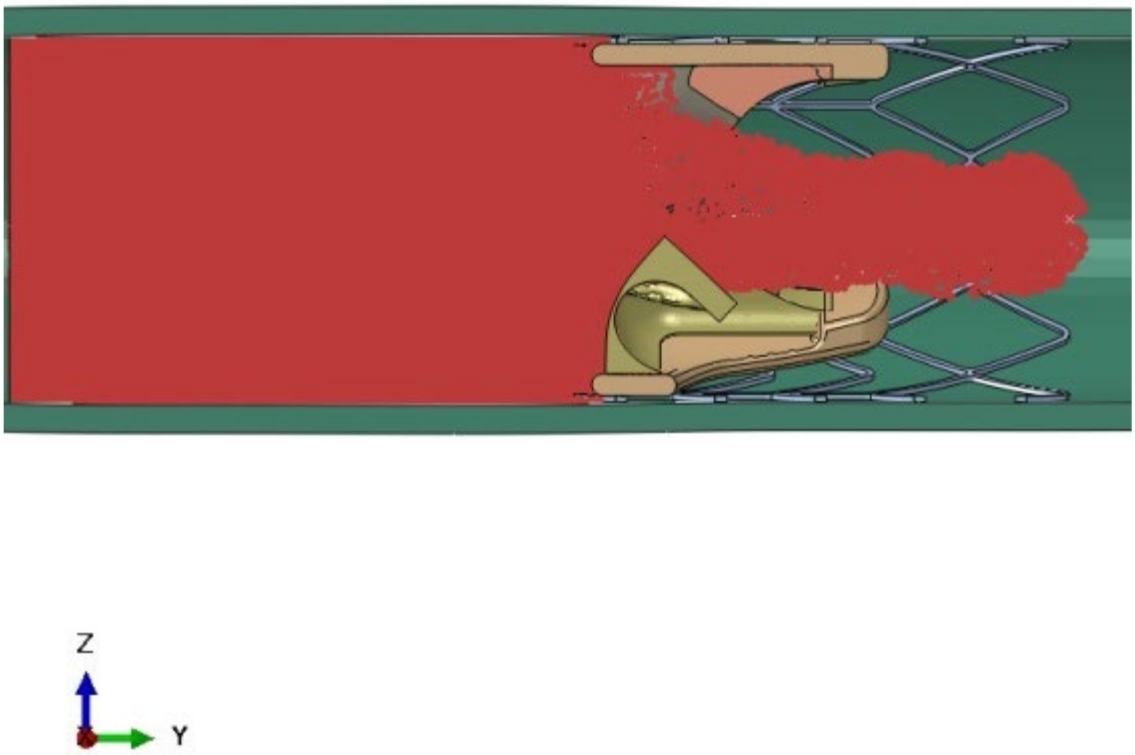

c.

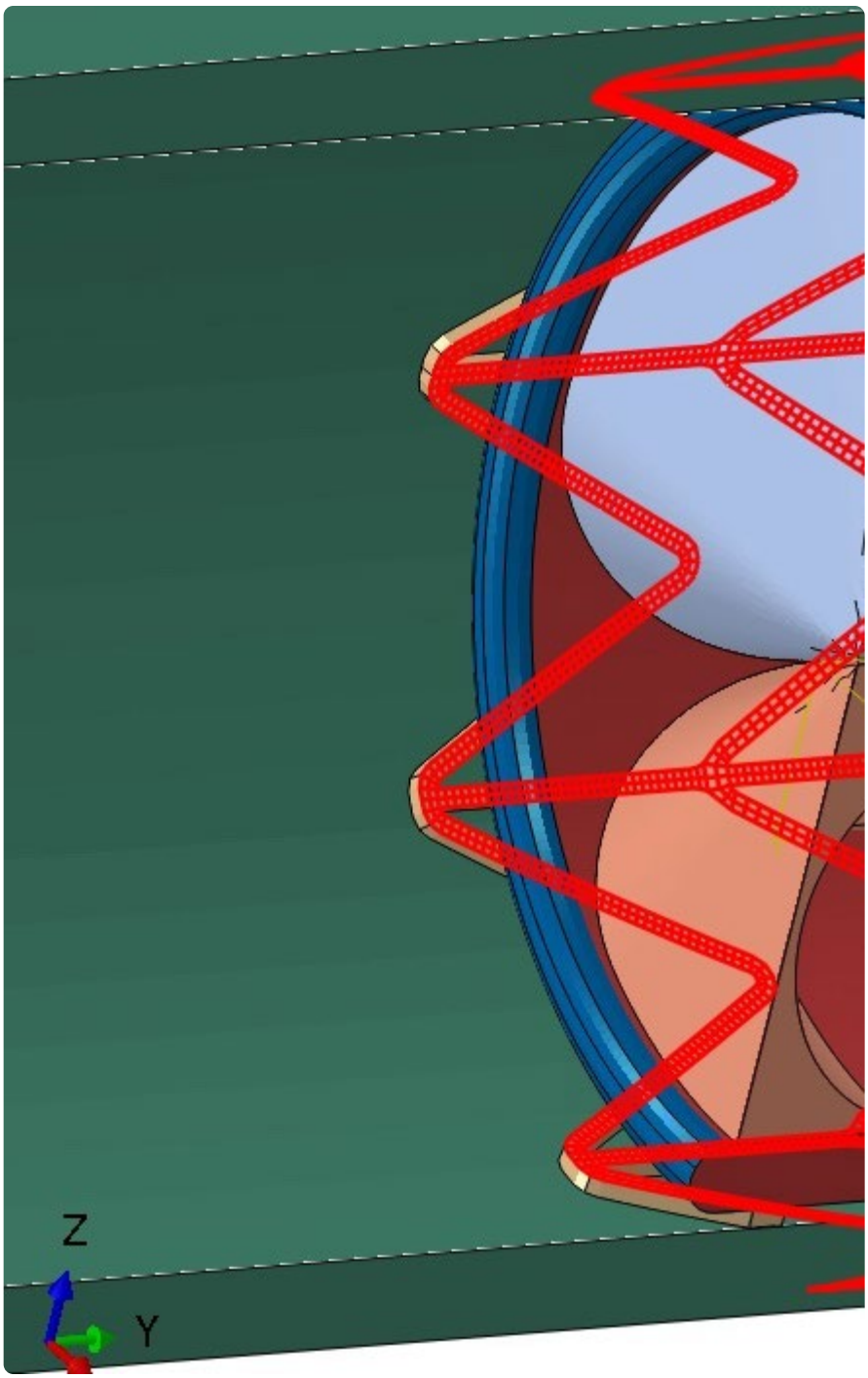

Table 1

NiTinol material model [3]

Density kg/m^3	Austenite		Martensite							
	Young Modulus	Poisson Ratio	Young Modulus	Poisson Ratio	Trans. Strain	Start of trans.	End of trans.	Start of trans.	End of trans.	En Co

	(MPa)		(MPa)			Loading (MPa)	Loading (MPa)	Unloading (MPa)	Unloading (MPa)	Lo (M
6412	46728	0.33	25199	0.33	0.0426	356.82	437.80	124.50	17.75	53

$$U=\sum_{i=1}^{N}\frac{2\mu_i}{\alpha_i^2}\left(\bar{\lambda}_1^{\alpha_i}+\bar{\lambda}_2^{\alpha_i}+\bar{\lambda}_3^{\alpha_i}-3\right)+\sum_{i=1}^{N}\frac{1}{D_i}\left(J^{el}-1\right)^{2i},$$

$$\mu_0=\sum_{i=1}^{N}\mu_i\,,\qquad K_0=\frac{2}{D_1}.$$

Figure 4

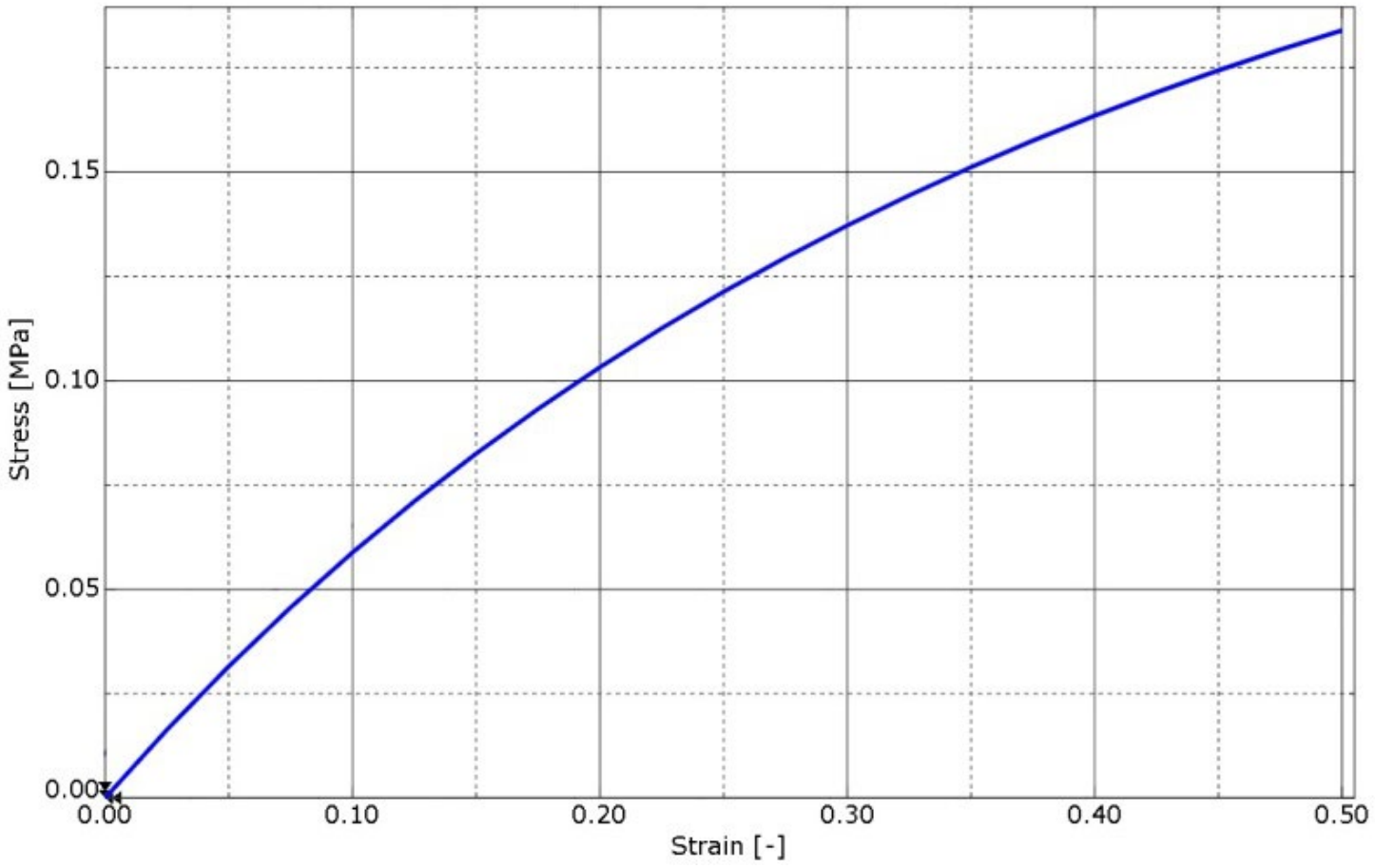

Uniaxial Stress-Strain curve of Hyperelastic Ogden 2nd order material model

$$\langle f(\mathbf{x})\rangle\simeq\sum_j\frac{m_j}{\rho_j}f_jW\left(|\mathbf{x}-\mathbf{x}_j|,h\right).$$

Figure 5

Stress [MPa] distribution in the valve and stent for both loading cases: 1: the pressure load (a,c) and 2: fluid-structure interaction (b,d)

a.

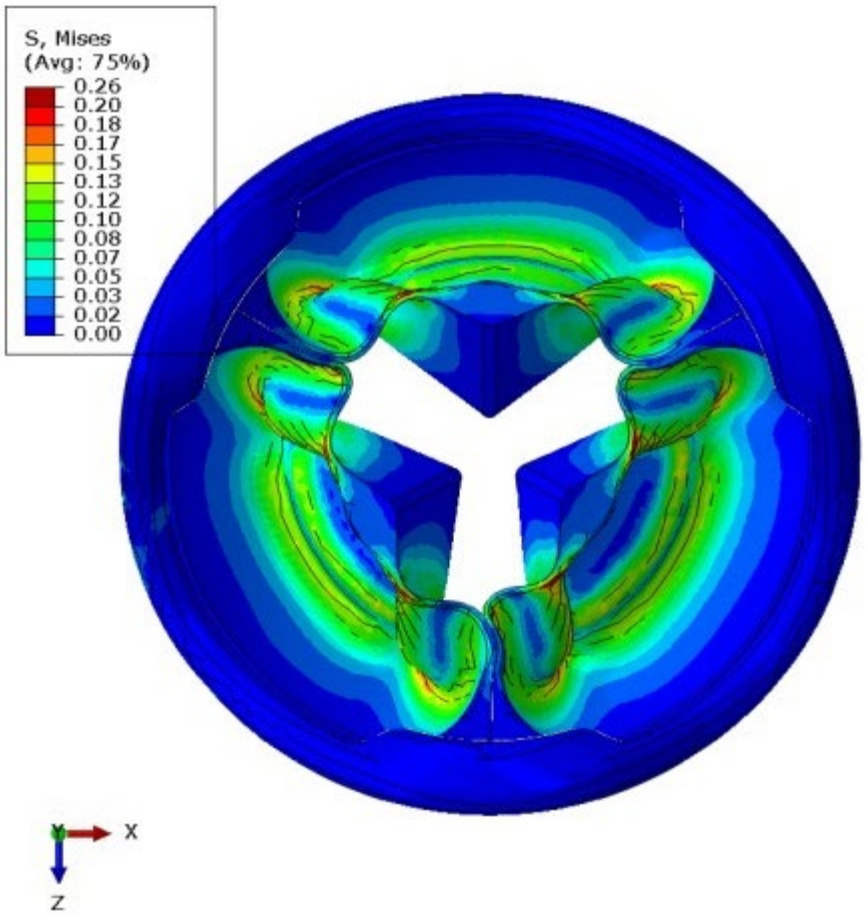

b.

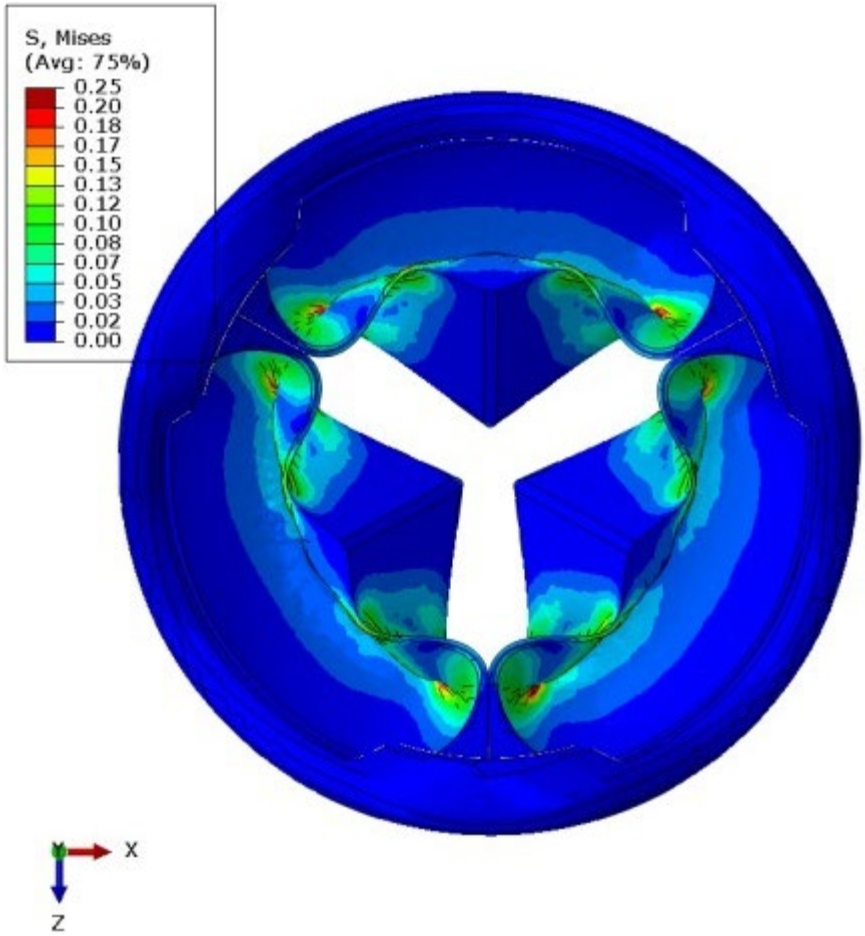
S, Mises
(Avg: 75%)
0.25
0.20
0.18
0.17
0.15
0.13
0.12
0.10
0.08
0.07
0.05
0.03
0.02
0.00
X
Z

C.

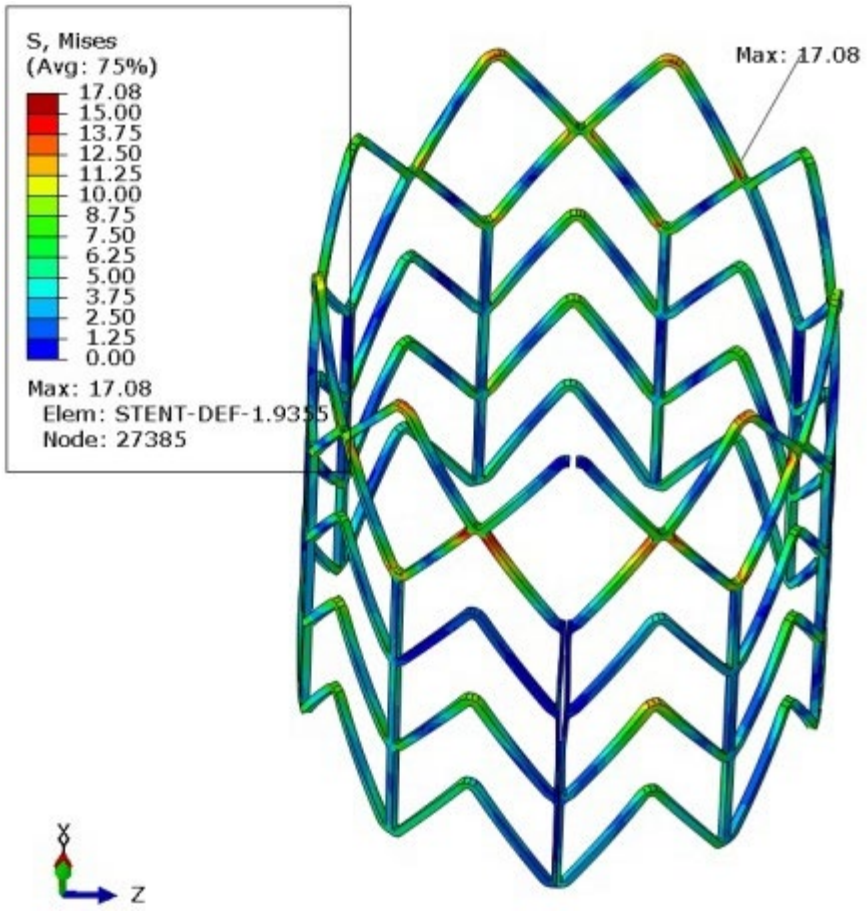
S, Mises
(Avg: 75%)
17.08
15.00
13.75
12.50
11.25
10.00
8.75
7.50
6.25
5.00
3.75
2.50
1.25
0.00
Max: 17.08
Elem: STENT-DEF-1.9355
Node: 27385
Max: 17.08
Y
Z

d.

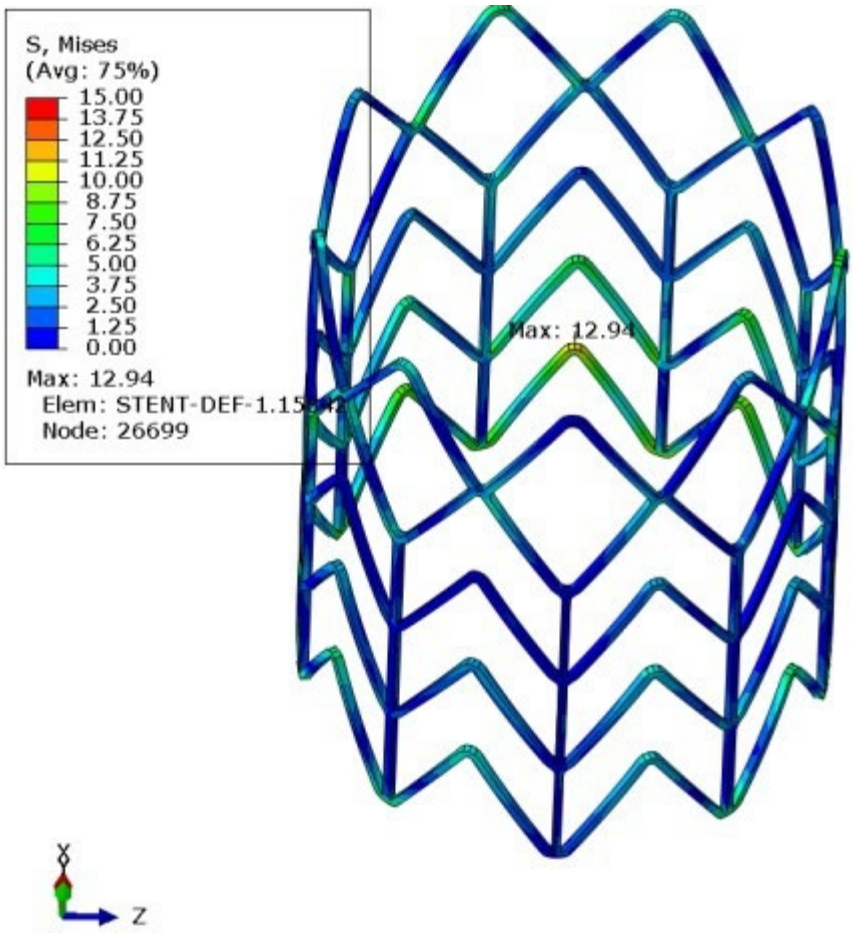

Figure 6

Radial Deformation [mm] for loading case 1 (a,c) and loading case 2 (b,d), using a 10x scale for a better visualization

a.

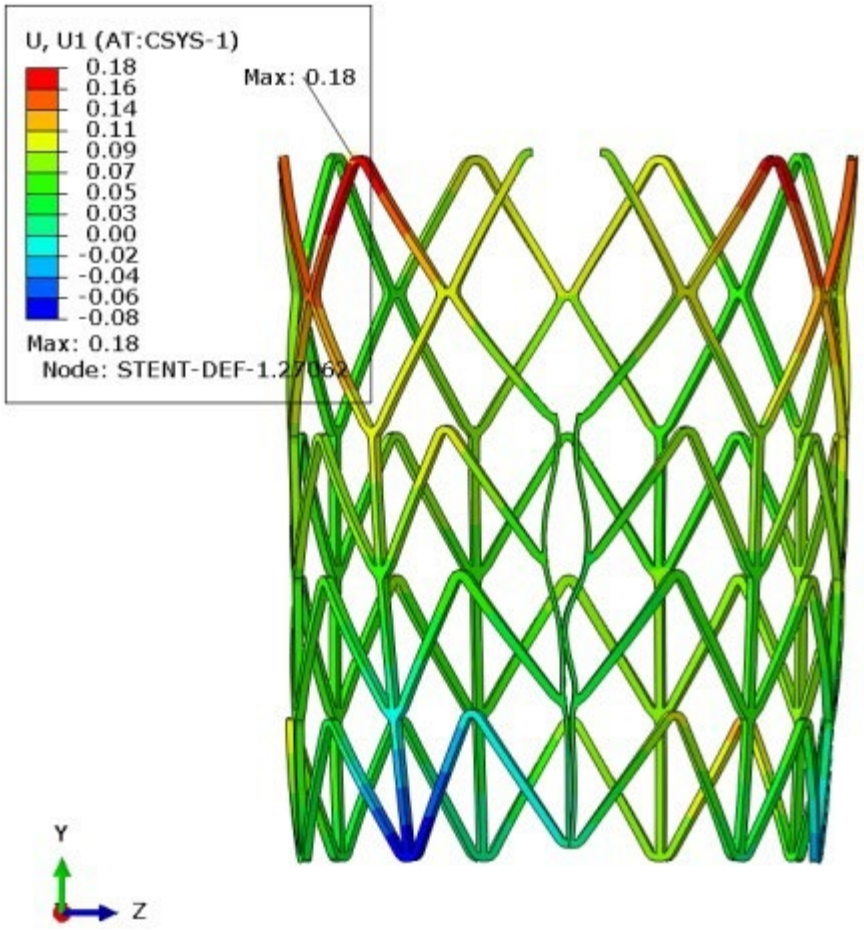
U, U1 (AT:CSYS-1)
0.18
0.16
0.14
0.11
0.09
0.07
0.05
0.03
0.00
-0.02
-0.04
-0.06
-0.08
Max: 0.18
Max: 0.18
Node: STENT-DEF-1.27062
Y
Z

b.

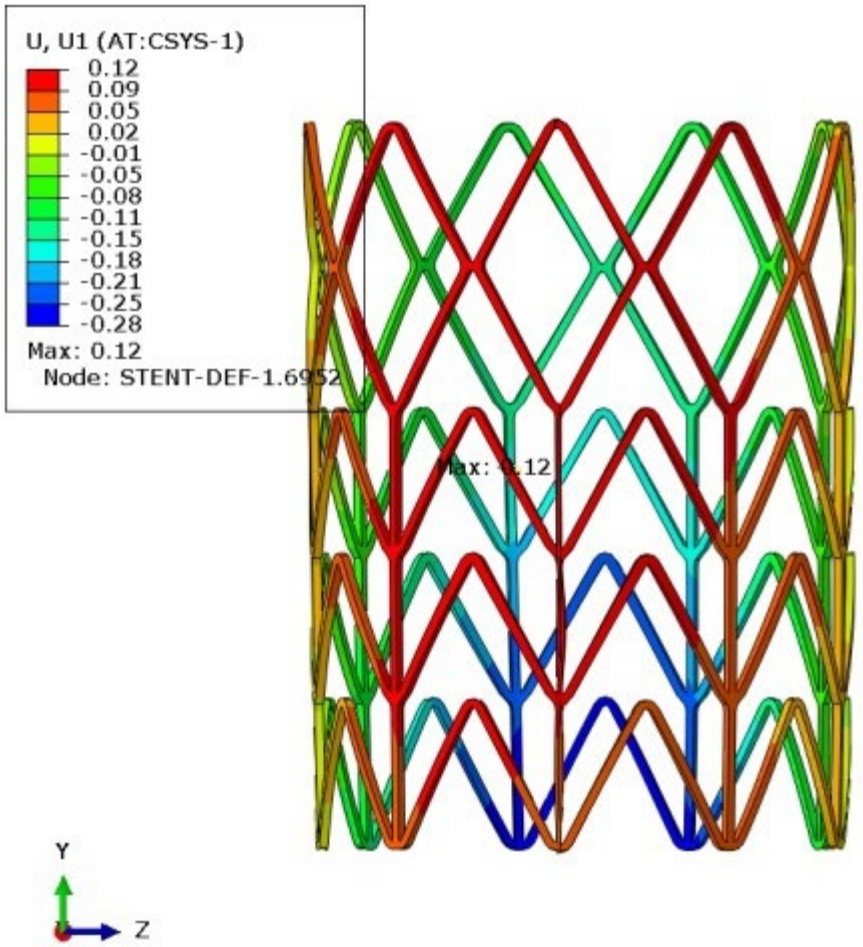
U, U1 (AT:CSYS-1)
0.12
0.09
0.05
0.02
-0.01
-0.05
-0.08
-0.11
-0.15
-0.18
-0.21
-0.25
-0.28
Max: 0.12
Node: STENT-DEF-1.6952
Y
Z

C.

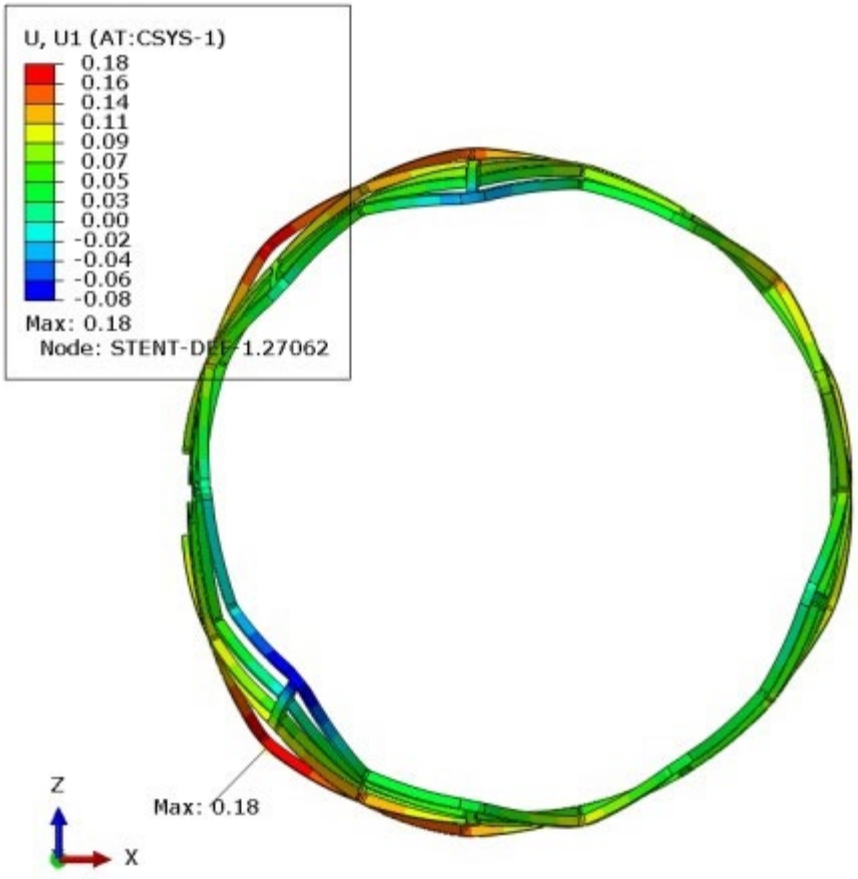
U, U1 (AT:CSYS-1)
0.18
0.16
0.14
0.11
0.09
0.07
0.05
0.03
0.00
-0.02
-0.04
-0.06
-0.08
Max: 0.18
Node: STENT-DEF-1.27062
Z
X
Max: 0.18

d.

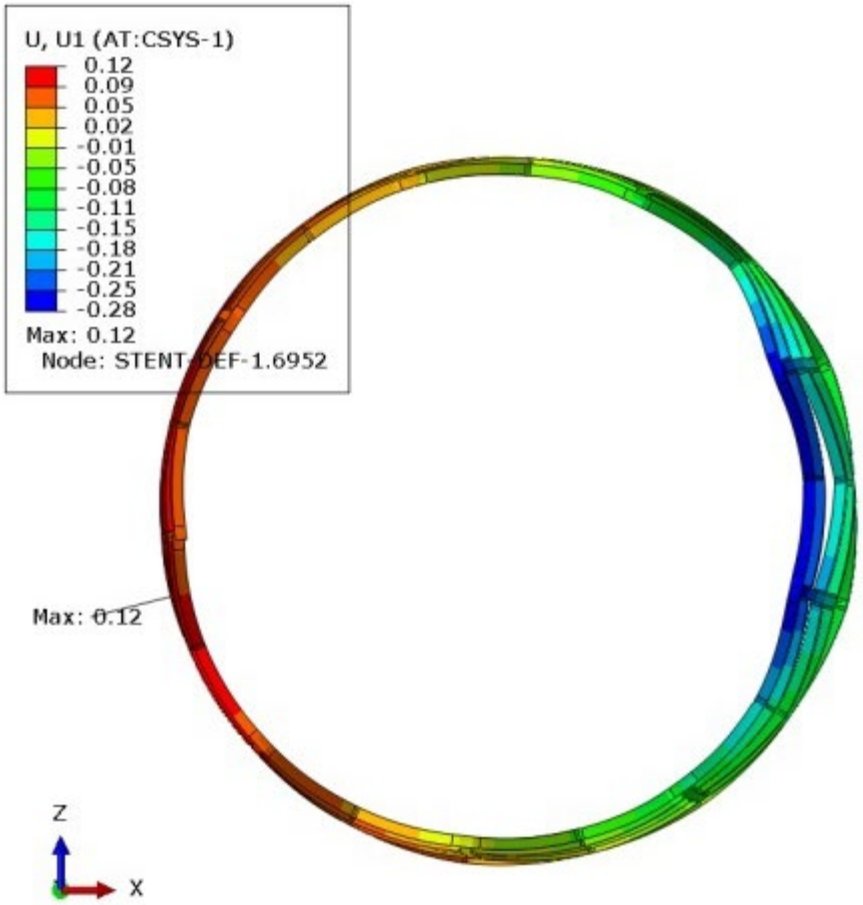

Figure 7

Axial Deformation [mm] for loading case 1 (a) and loading case 2 (b), using a 10x scale for a better visualization

a.

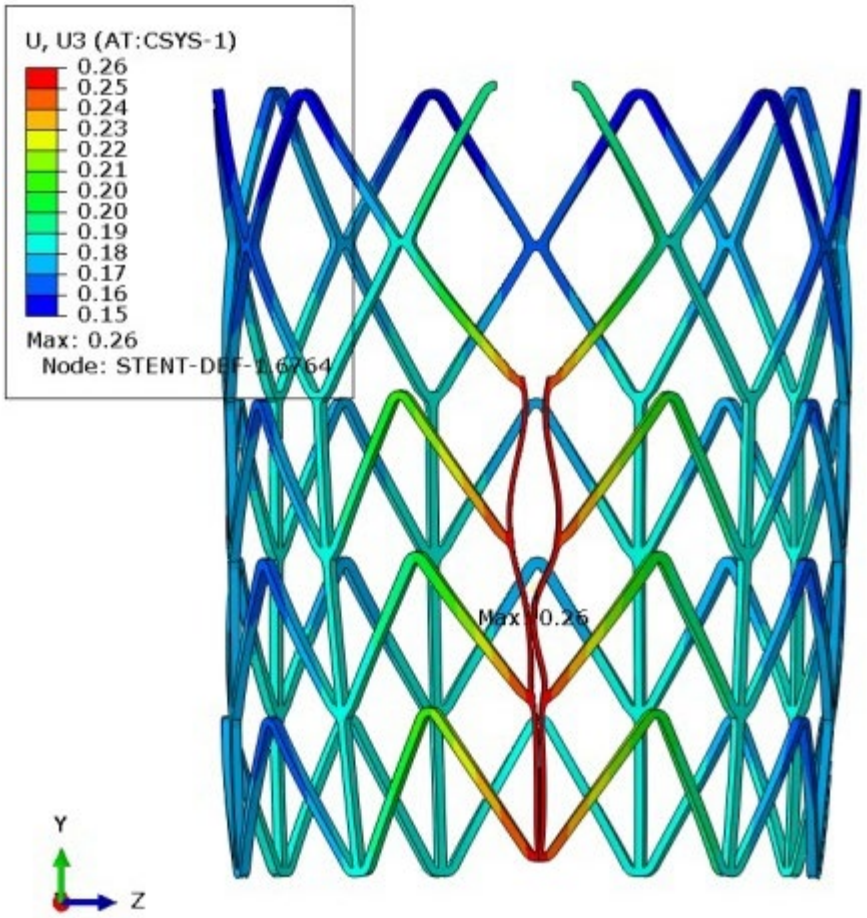
U, U3 (AT:CSYS-1)
0.26
0.25
0.24
0.23
0.22
0.21
0.20
0.20
0.19
0.18
0.17
0.16
0.15
Max: 0.26
Node: STENT-DEF-1.67764
Max: 0.26
Y
Z

b.

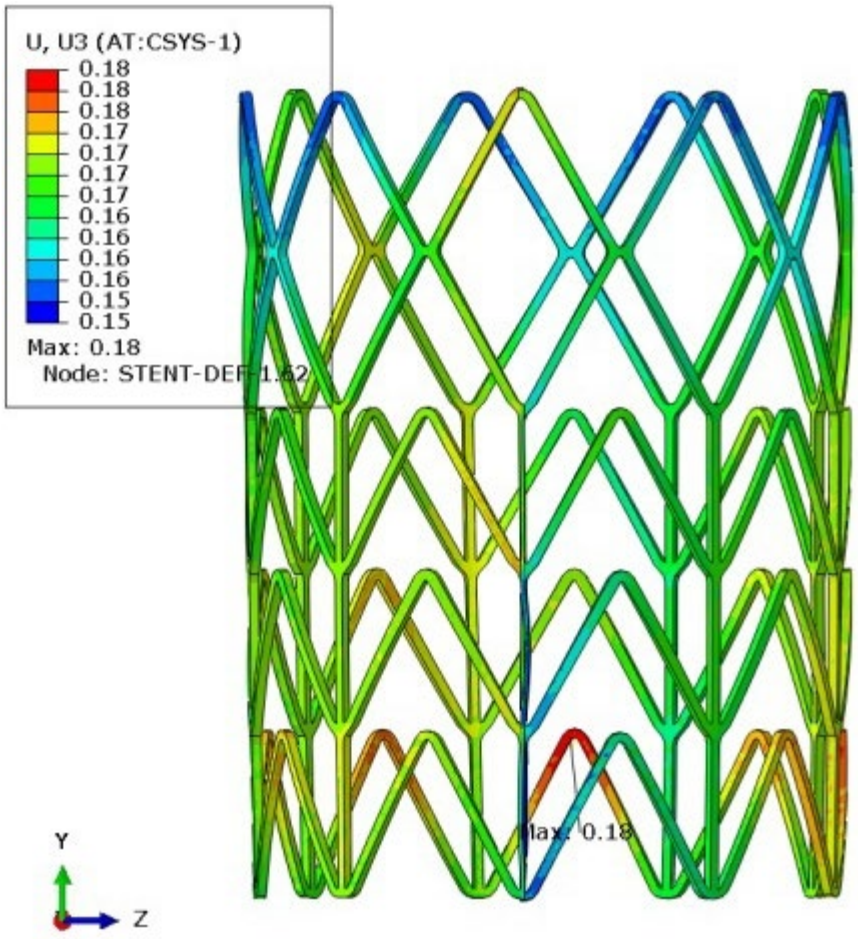
U, U3 (AT:CSYS-1)
0.18
0.18
0.18
0.17
0.17
0.17
0.17
0.16
0.16
0.16
0.16
0.15
0.15
Max: 0.18
Node: STENT-DEF-1.62
Max: 0.18
Y
Z